MODEL-BASED OPTIMIZATION AND ADAPTIVITY OF CRICKET-INSPIRED BIOMIMETIC ARTIFICIAL HAIR SENSOR ARRAYS

R. K. Jaganatharaja, N. Izadi, J. Floris, T. S. J. Lammerink,
R. J. Wiegerink and G. J. M. Krijnen
Transducers Science & Technology group, MESA+ Research Institute,
University of Twente, P.O. Box 217, 7500 AE Enschede, The Netherlands.
r.kottumakulal@ewi.utwente.nl

Abstract *— We present a model for our cricket-inspired, biomimetic, artificial hair sensors, to analyze the sensitivity dependence on structural and geometrical parameters. Based on this model, feasible design improvements to achieve an increased sensitivity are discussed and a figure of merit to evaluate sensor performance is defined. Also, we discuss the results of a novel approach to implement adaptive sensor arrays through DC-biasing based on the electrostatic spring-softening effect. Experimental results show a clear theoretical accordance and tunability of system's resonance frequency, providing opportunities for frequency focusing and selective sensitivity.*

Key Words: *biomimetics, flow-sensors, adaptation, artificial hair sensors, spring-softening, capacitive sensors*

I INTRODUCTION

Crickets have, quite often, been a subject of common interest to biologists and engineers. They have evolved with a pair of special flow-sensitive appendices called cerci with numerous mechano-receptive filiform hairs of different lengths, distributed on the surface. These filiform hairs are extremely sensitive to acoustic signals, down to thermal noise levels [1], enabling them to identify and escape from approaching predators. Each filiform hair has a mechano-sensitive neuron at its base which fires a neuro-signal whenever there is a flow-induced deflection on the hair, see Figure 1.

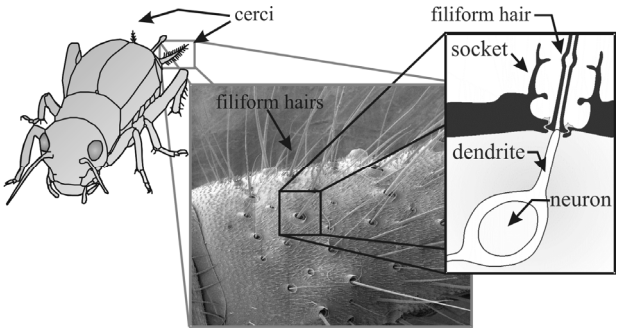

Figure 1. Mechano-receptive hairs found on cerci of crickets [*SEM image courtesy by Jerome Casas, IRBI, Université de Tours.*]

Inspired by crickets and making use of technical advancements in MEMS techniques, SU-8 based artificial hair sensor arrays were successfully implemented recently [2]. Ways to improve the sensitivity of these artificial hair sensor arrays have been demonstrated; increasing the hair length and arranging the sensors on an artificial cercus-like platform that can be assembled to facilitate 3D-flow sensing, see Figure 2.

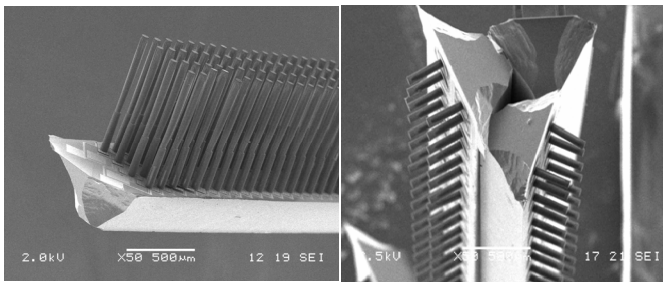

Figure 2. SEM images of the realized biomimetic hair sensor arrays, arranged on the artificial cerci-like substrate.

In this work, we present a model for our artificial hair sensor to further study and optimize the effects of structural and geometrical parameters on the sensitivity and a figure of merit for our sensors is defined based on this model. Parallel to this, we present a new approach to develop adaptive hair sensors which are tunable with respect to the best frequency and sensitivity [3]. Possible design improvements aimed at increased sensitivity are discussed.

II PRINCIPLE OF OPERATION

The artificial hair sensor is based on a differential capacitive sensing technique. Drag-torque due to the air flow, picked-up by the SU-8 hair, results in a membrane tilt. This flow-induced tilting of silicon nitride (SiRN) membrane with electrodes on top, causes a change in the sensor capacitance, with

respect to the bottom electrode (bulk silicon), see Figure 3. The capacitance change is read-out using charge amplifiers and synchronous detection [2].

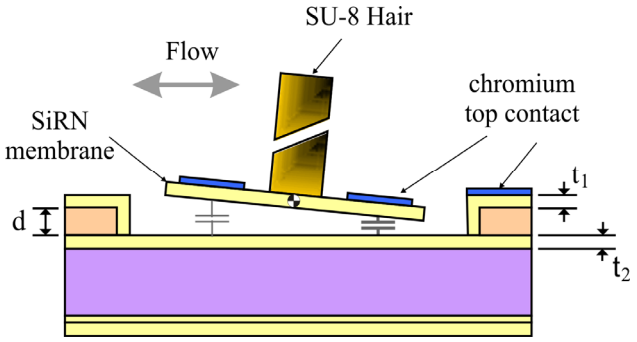

Figure 3. Schematic of the hair sensor

III SENSOR MODEL

The structural functionality of cricket hairs has been described in terms of mechanical and hydrodynamic models in literature [4,5]. Whereas biologists have used the models to arrive at estimates of the mechanical properties of the hairs (hair moment of inertia J, torsional spring constant S and torsional resistance R), we have implemented the model to optimize our sensor design with respect to actual sensor properties.

The normalised sensitivity dC/dV_0 (C the capacitance and V_0 the far field flow velocity amplitude) can be approximated by the product of: (i) the hydrodynamic torque pick-up by the hairs, (ii) the second-order mechanical system response, and (iii) the capacitance change per unit of rotation of the membrane (F/rad) [3]. The approximation lies in assuming that the velocity of the tip of the hairs is much smaller than the flow velocity itself.

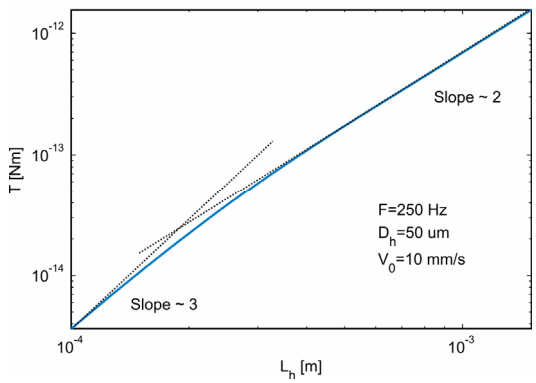

Figure 4. Drag-torque on hairs, vs. hair length (model).

Using the model we investigated the dependence of the sensitivity as a function of hair-length (Figure 4). Calculation of the flow-induced drag-torque on the hairs is based on Stokes' drag formulations [4]. The drag-torque increases approximately proportional to the hair length cubed $(L_h)^3$, when L_h is smaller than the boundary layer thickness (δ) and with approximately $(L_h)^2$ when $L_h>\delta$. On the other hand, changing the diameter of the hairs is by far not as influential.

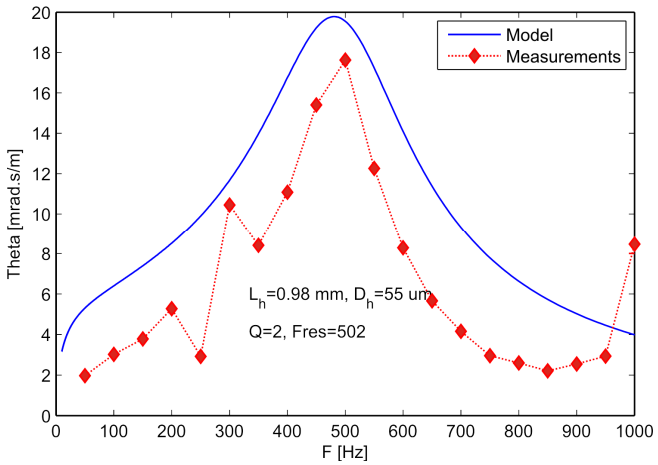

Figure 5. Measured (optically) and modelled normalized sensitivity of realized hair-sensors Vs. frequency.

Experimental results were obtained using a laser-vibrometer and acoustic excitation by a small loudspeaker in the very near field [6]. For comparison the model-results are shown in Figure 5. The only chosen parameter in these calculations is the quality factor, other values (J, S, T_{drag} etc) were directly obtained from the hydro-dynamics and structural properties. Model and measurements are in good agreement both with respect to the frequency dependence and to the absolute sensitivity values.

FIGURE OF MERIT (FOM)

Sensor-optimization has (at least) two dimensions: bandwidth and (low-frequency) sensitivity. Using the results of the model, a figure of merit (FOM) is defined as the usable bandwidth (i.e. the resonance frequency) times the drag-torque pick-up. Hence:

$$FOM \equiv \sqrt{\frac{S}{\rho L_h^3 D_h^2}} \cdot \frac{L_h^2 D_h^{1/3}}{S} = L_h^{1/2} \cdot (\rho S)^{-1/2} \cdot D_h^{-2/3} \qquad (1)$$

Sensitive sensors with a large usable bandwidth should have long, thin hairs made of low density material, and small torsional stiffness, exactly what is seen in nature. In comparing the FOM of our sensors to the FOM of crickets, taking data from [4], we find that the ratio is about 78 for hairs of 1 mm length. Crickets out-perform the artificial sensors because of their low torsional stiffness

($2\cdot10^{-11}$ vs. $1\cdot10^{-8}$ nm/rad) and small hair-diameter (8.2 vs. 50 µm) giving clear directions for further optimisation of our sensors.

IV ADAPTIVITY

ELECTROSTATIC SPRING SOFTENING

Based on transduction theory, applying a bias voltage on the capacitors results in a change in the effective spring stiffness, given as:

$$S_{eff} = S_0 - \frac{U_{bias}^2}{2}\frac{\partial^2 C}{\partial \alpha^2} = S_0 - U_{bias}^2 \kappa \qquad (2)$$

Where S_{eff} is the effective spring constant, α is the sensor plate angular rotation, S_0 is the physical rotational spring stiffness of the torsional beams, U_{bias} is the applied bias voltage, C is the capacitance of the device and κ is the second derivative of the capacitance with respect to the angle of rotation divided by two.

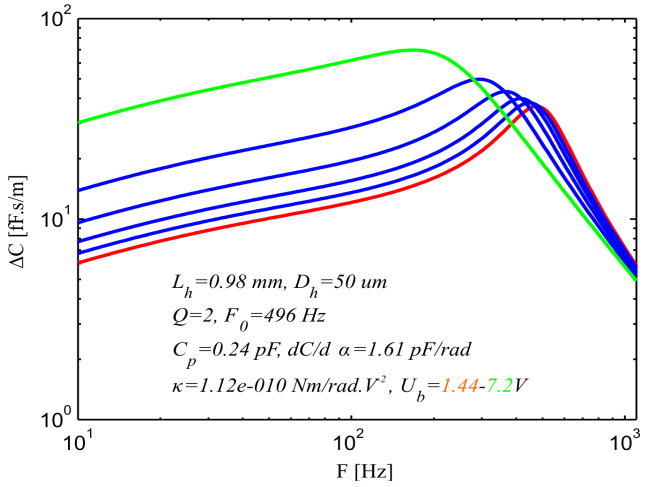

Figure 6: Model predictions showing the adaptive behavior of sensitivity and resonance frequency for a range of applied bias voltages (U_{bias} = 1.44 – 7.2 V)

Since U_{bias}^2 is always positive, an applied bias voltage will give a reduction in the spring stiffness. Therefore DC-biasing results in increasing the tilt angle, at given drag-torque acting on the hairs (and for frequencies below the best frequency), given by:

$$\alpha = \frac{T(\omega, V_0)}{S_{eff}} = \frac{\alpha_0}{1 - \frac{\kappa}{S_0} U_{bias}^2} \qquad (3)$$

where T is the total drag torque acting on the hair (depending on frequency ω and far-field velocity amplitude V_0) and α_0 is the angle of rotation for given T without applied DC-bias. By the relation between resonance frequency and spring stiffness, the change in the resonance frequency, ω_0, by DC-biasing is given as:

$$\omega_0(U_{bias}) = \sqrt{\frac{S(U_{bias})}{I}} = \omega_0(0)\sqrt{1 - \frac{\kappa}{S_0} U_{bias}^2} \qquad (4)$$

Here κ/S_0 is a constant depending on the geometry of the structure. From Eqn. (3) and (4) it follows that the hair-sensors can be adaptively changed to accommodate optimal signal reception (Figure 6). In order to estimate the sensitivity to DC-biasing we calculated the coefficient κ. In general this coefficient cannot easily be calculated analytically for any non-zero α. However, in the case of the hair sensors studied here, with small angles of rotation encountered in practice, κ is calculated as in Eqn. (6) where g is the effective dielectric spacing between the capacitor electrodes and A the surface area of the electrodes.

$$\kappa = \frac{\partial^2}{\partial \alpha^2}\left(\frac{1}{2}\int_A \frac{\varepsilon_0 dA}{g(x,y,\alpha)}\right) \approx \lim_{\alpha \to 0} \frac{1}{2}\int_A \frac{\partial^2}{\partial \alpha^2}\left(\frac{\varepsilon_0}{g(x,y,\alpha)}\right) dA \qquad (5)$$

Using Eqn. (6) we find for a stress-induced curved circular membrane, with radius R and maximum deflection a at the rim:

$$\kappa = \frac{\pi \varepsilon_0}{8a} R^4 \left\{\frac{1}{t_{eff}^2} - \frac{1}{(t_{eff} + a)^2}\right\} \qquad (6)$$

Where $t_{eff}=d+(t_{SiRN})/\varepsilon_r$, d is the airgap and t_{SiRN} is the total SiRN thickness in the capacitors.

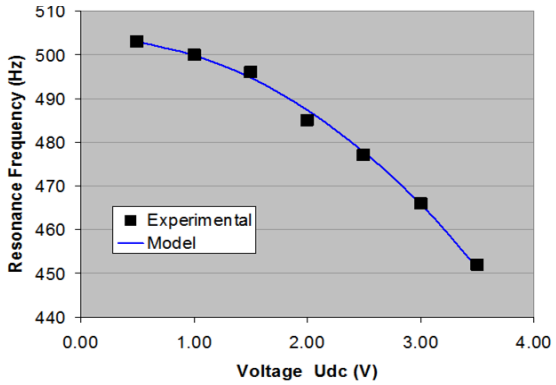

Figure 7. *Resonance frequency vs. applied DC-bias. Solid line is the model fitted (U_{bias}=0).*

EXPERIMENTS AND RESULTS

In order to verify the model predictions on DC-biasing, two types of experiments were conducted:

(1) With the electrical actuation DC-bias voltages were applied and resonance frequencies were determined. Figure 7 shows the measured resonance frequencies for the sensor at different applied DC-bias voltages and the solid line is the model, Eqn. (4), fitted to the measurement data using $U_{bias} = 0$, resulting in a value for κ/S_0 of 0.016 V^{-2}.

(2) With the acoustic actuation, a loudspeaker was used to apply the airflow and the sensors were placed in the very near field of a loudspeaker. The membrane rotation normalized to the air flow, at various DC-bias voltages was characterized using a laser vibrometer. Figure 8 gives the membrane's maximum angle of rotation normalized to the applied air flow from the loudspeaker versus the bias voltage at various actuation frequencies. Fitting the measurement data to the model, Eqn. (3), we find a value for κ/S_0 of 0.0171 V^{-2}.

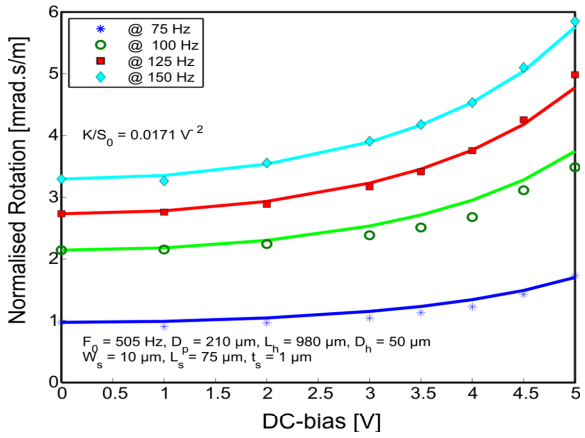

Figure 8. ***Normalized membrane rotation by a sinusoidal flow, vs. DC-bias. Parameters are indicated in the figure.***

Using the model, the calculated value of κ/S_0 based on the geometrical and material parameters of the sensors (i.e. without any fit), was 0.0156 V^{-2}, which proves that model's predictions are relatively close to the experimental values.

ELECTRODE OPTIMIZATION

The sensitivity and adaptivity of the sensors depend mainly on the design and the quality of the fabricated membrane. Present sensors suffer from membrane curvature due to residual stress in the chromium electrode layer, reducing sensitivity. Membrane curvature can be decreased by reducing the electrode area near the rotational axis. The influence of this approach on the sensitivity and the coefficient κ was analyzed. Figure 9 shows the sensitivity and κ versus the reduction in electrode area. Both sensitivity and adaptivity are seen to increase with reduced electrode area up to a certain optimum.

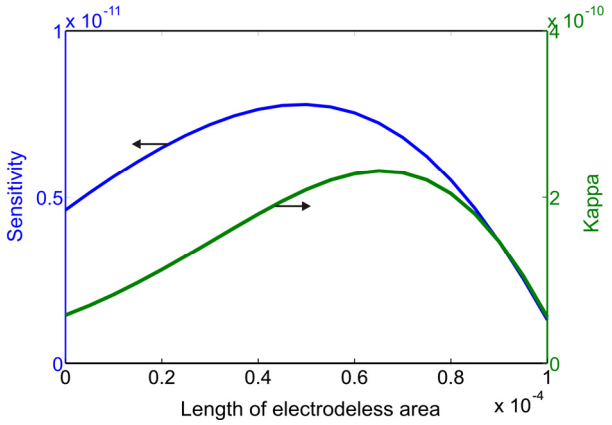

Figure 9. ***Sensitivity and coefficient κ (adaptivity) vs. reduction in the electrode area.***

V CONCLUSION

A model-based optimization scheme and a figure of merit to evaluate sensor performance have been presented. Experimental results correspond well to model predictions. Adaptivity of the sensor based on electrostatic spring softening by DC-biasing has been described and experimentally shown, with good theoretical agreement. A design improvement for the electrodes is suggested.

ACKNOWLEDGEMENTS

The authors want to thank: Meint de Boer, Erwin Berenschot, and Dominique Altpeter, for their advices on processing of the devices and also our colleagues in the EU project CILIA for their stimulating discussions and inputs to this work.

REFERENCES

[1] T. Shimozawa *et al*, *"Sensors and Sensing in Biology and Engineering"*, Vienna, ed. Barth, Humphry and Secomb (Springer), Chapter 10, 2003.

[2] Dijkstra et. al, "Artificial sensory hairs based on the flow sensitive receptor hairs of crickets", *J. Micromech. Microeng,*. Vol. 15**,** pp. S132–S138, 2005.

[3] G.J.M. Krijnen *et al.*, "Biomimetic micromechanical adaptive flow sensor arrays", *SPIE* Microtechnologies for the New Millennium, May 2007, Maspalomas, Gran Canaria, Spain, *Proceedings Vol. 6592.*

[4] T. Shimozawa, et al,, "Structural scaling and functional design of the cercal wind-receptor hairs of cricket", *J. Comp. Physiology*, Vol. 183, pp. 171-186, 1998.

[5] J. Humphrey et al, "Dynamics of arthropod filiform hairs. II. Mechanical properties of the hair and air motions", *Philosophical Transactions: Biological Sciences*, Vol. 340, Nr. 1294, pp. 423-444, 1993.

[6] H-E. de Bree et al. 11th Int. Cong. on Sound and Vibration (ICSV11), St. Petersburg 2004.